https://doi.org/10.1016/j.jcsr.2021.106930

Experimental investigation on recycled aggregate concrete filled steel tubular stub columns under axial compression

Vanessa da S. de Azevedo[1], Luciano R. O. de Lima[2], Pedro C. G. da S. Vellasco[2], Maria E. da N. Tavares[2] and Tak-Ming Chan[3]

[1] PGECIV - Civil Engineering Post-Graduate Program, UERJ – State University of Rio de Janeiro, Brazil

[2] Structural Engineering Department, UERJ – State University of Rio de Janeiro, Brazil

[3] Department of Civil and Environmental Engineering, The Hong Kong Polytechnic University, Hong Kong

Abstract: This paper presents an extensive experimental investigation of the circular recycled aggregate concrete filled steel tubes (RACFST) stub columns under to axial compression to assess their cross-section behaviour. Recycled aggregate concrete is a sustainable concrete produced with recycled coarse aggregate (RAC) from demolition wastes generally used to fabricate non-structural elements. When compared with natural coarse aggregate (NCA), the recycled coarse aggregate presents lower mechanical properties due to physical and chemical changes that occurred during the recycling process, and thus the resulting RAC possess lower strength than the conventional natural aggregate concrete. However, the confinement provided by the circular steel tube can increase the strength and ductility of RAC in recycled aggregate concrete filled steel tubes (RACFST) columns. The test programme presented in this paper comprised twenty-three composite columns with replacement ratios (the mass percentages of the NCA replaced by RCA in concrete) corresponding to 0% (nature coarse aggregate), 30 and 50% (recycled aggregate concrete), plus four steel columns used for comparison. The experiments have shown that, as anticipated, the concrete core enhances the composite section load-carrying capacity. However, the control over the contents of this concrete core influences the composite section's ductility. If the fill material presents a brittle behaviour, stress redistributions occur in both steel and concrete to compensate for this effect. Since the behaviour of natural aggregate concrete filled steel tubes (NACFST) and RACFST columns are similar, the present

paper starts from a study based on a comparative assessment of the recommendations presented in ABNT NBR 8800, ABNT NBR 16239, AISC 360-16, Eurocode 4 and Australian/New Zealand AS/NZS 2327 design standards. These design recommendations proved to be consistent and in line with the performed experiments. Additionally, the results indicated that the cross-section slenderness ratio (D/t) and the confinement ratio directly influence the composite section response.

Keywords: composite columns, recycled aggregate concrete, experimental analysis, sustainability.

1. Introduction

Composite columns are characterised by having a “wrap” on a concrete core. The first category comprises the cases in which rolled or welded steel profiles are involved in a concrete region. The second involves tubular cross-sections filled with concrete. Generally additional reinforcement bars are only needed in columns with large steel cross-sections and serve to increase the strength of the composite section, as can be observed in Figure 1. A large part of the steel structures requires a protective layer around the steel sections to guarantee adequate fire resistance and durability. The composite solution is a natural consequence of these requirements since it combines fire protection and durability aspects while also increasing its structural resistance. These facts lead, in many cases, to structures that are more economical than their standard counterparts.

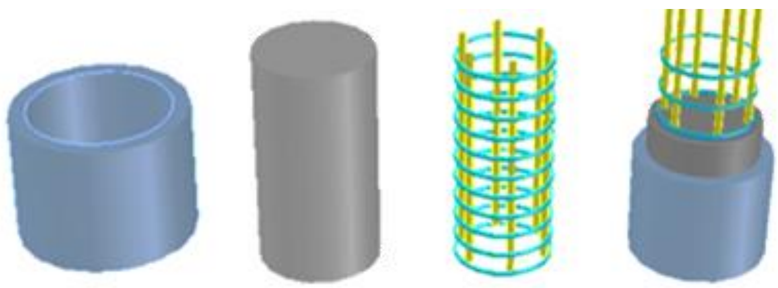

Figure 1. Reinforced concrete-filled steel tubular columns – RCFST.

Besides presenting a more adequate visual and aesthetic appearance, the composite tubular sections also provide other structural advantages related to the concrete confinement and the composite section fire resistance, strongly dependent on the concrete core strength. Composite columns' response has been widely investigated in the last decades, firstly involving steel shapes encased in concrete as investigated by Mirza [1]. Afterwards, experimental and numerical investigations were also assessed using concrete-filled steel tubes, indicating that the strength and ductility decreased as the diameter to thickness (D/t) ratios increased. This conclusion was confirmed by tests that showed the load and bond conditions significantly influenced their axial load behaviour, [2], [3], [4]. Additionally, the influence of the concrete compressive strength up to 100 MPa in the CFST's behaviour has also been investigated by Ellobody et al. [5], Gupta et al. [6] and Yu et al. [7]. The authors concluded that the column strengths increase is directly proportional to the concrete cube strength. On the other hand, the concrete confinement provided by the steel tube may also increase the CFST's strength since the load when the confinement starts is higher than the sum of the steel and concrete individual contribution, as reported by Susantha et al. [8], Oliveira et al. [9] and Yan et al. [10]. It could also be observed that for smaller D/t ratios, the steel tube provides a good confinement for the concrete. Giakoumelis and Lam [11] observed that Eurocode 4 (EC4) provides a good prediction of the axial strength of CFST columns with a mean ratio of 1.17 between the experimental and calculated axial capacities. The experimental and predicted axial strength ratios using ACI 318-95 [12] and AS3600 [13] and AS4100 [14] were approximately equal to 1.35, showing a certain level of conservatism. These statements were also supported by Chitawadagi et al. [15] based on experiments involving CFSTs with various cross-sections slenderness (D/t) and different grade concrete grades and numerical results provided by Zhao et al. [16].

The last few years presented an increase of investigations with CFST columns with high strength steel (up to 780 MPa) and concrete with high compression cylinder strength (up to 190 MPa), i.e. Liew et al. [17], [18], Uy et al. [19] and Yan et al. [20]. The authors concluded that the current EC4 method could be safely extended to CFST members design with steel strength up to 550 MPa and concrete compressive cylinder strength up to 190 MPa, with minor modifications and restrictions. Finally, Han et al. [21] provided an in-depth discussion on the recent advances and developments in applications of concrete-filled steel tubular structures in the last decades, emphasising the composite action between steel tube and filled concrete and its alternative steel or the reinforced concrete systems.

Around the world, the construction industry produces large quantities of construction and demolition waste every day, indicating the high demand for potential use of demolition waste [22]. Recycling of waste concrete is beneficial and necessary for environmental preservation and effective utilisation of resources. Effective utilisation of concrete waste is created by using it as recycled aggregates for concrete production. To make this technology feasible, a significant number of experiments has been carried out. Various investigations mainly engaged in the processing of demolished concrete, the mixture design, the physical and mechanical properties, and the durability aspects [23].

These investigations, focused on structural capacity and sustainability aspects, have grown since the 2000s as composite columns use recycled aggregate concrete. Xiao et al. [23] investigated the compressive strength and the stress-strain curves of recycled aggregate concrete (RAC) with different replacement percentages of recycled coarse aggregate (RCA) of 0%, 30%, 50%, 70% and 100%, respectively. The authors concluded that the compressive strengths of RAC, generally decrease as the RCA contents increase. They also indicated that the RAC elastic modulus is lower than in standard concrete. For example, for a RCA replacement percentage equals to 100%, the elastic modulus is reduced by 45%. One of the first investigations in recycled aggregate composite columns was carried out by Konno et al. [24]. The authors concluded that the deformation behaviour of recycled aggregate concrete-filled steel tube (RACFST) resembled the results associated to standard concrete-filled steel tubes (CFST). Similar conclusions were obtained by Wu and Yang [25], Yang and Han [26], Yang [27], Chen et al. [28], Tam et al. [29] and Wang et al. [30]. Xu et al. [31], based on extensive experimental and numerical simulations. The authors concluded that the additional water absorption of recycled aggregate concrete in manufacturing RACFST significantly influencing the compressive load-carrying capacity effect cannot be disregarded. Therefore, following sustainability requirements, some authors also investigated the use of recycled tyre rubber in concrete-filled steel tube columns of circular cross-section as performed by Silva et al. [32], [33] and Tao et al. [34].

The Brazilian design codes for composite columns ABNT NBR 8800 [35], ABNT NBR 16239 [36] and recycled aggregate concrete specifications ABNT 15116 [37] specifically deal with the use of recycled aggregates used in recycled concrete. However, it specifies that they involve no structural elements. According to these recommendations, the material was intended for uses such as fillers, subfloor, footbridges and the manufacture of non-structural elements, such as sealing blocks, curbs (guides), gutters, channels, posts and wall plates. With this scenario in mind, this paper aims to demonstrate the viability of using recycled aggregate concrete in composite columns changing the substitution ratio of the plain aggregate by recycled counterparts. The study was based on an experimental programme consisted of four steel columns and twenty-three composite columns. The specimens were made with different recycled coarse aggregate replacement percentages (RCA) of 0%, 30% and 50%. Afterwards, the experimental results were compared to the analytical formulations from current design specifications ABNT NBR 8800 [35], ABNT NBR 16239 [36], AISC 360-16 [38], Eurocode 4 [39], and Australian/New Zealand standard AS/NZS 2327 [40] to verify their applicability for RAFCST columns load-carrying capacity predictions.

2. Experimental programme

2.1 Tests overview

An experimental programme was developed to understand the structural behaviour of recycled aggregate concrete-filled steel tubular columns (RACFST), which included twenty-seven specimens [41]. The main objectives were to examine the cross-section behaviour and assess the influence of using RAC rather than standard concrete for the infill. Two different diameters were used in the first test series (152.4 mm) and the second test series (177.8 mm). The twenty-three composite specimens were divided according to the concrete compressive cylinder strength of 30 and 40 MPa varying the RCA replacement ratios (the mass percentages of the NCA replaced by RCA in concrete) corresponding to 0% (standard coarse aggregate), 30 and 50% (recycled aggregate concrete). Additionally, four steel hollow sections stub columns were also tested as a benchmark (identified as S1, S2, S3 and S4).

The columns' lengths were considered approximately three times the cross-section diameter to avoid flexural buckling. Still, they possessed a sufficient length to provide a good representation of the local imperfections and residual stress distributions [42]. The adopted nomenclature of each specimen series started with the letter S for steel cross-sections columns and C for composite columns, followed by the specimen ID, the steel tube diameter, the concrete compressive cylinder strength and the replacement ratio in percentage. For instance, C12-178-30-R30 corresponds to the twelfth composite column with a 178 mm diameter, a concrete compressive cylinder strength of 30 MPa and a recycled aggregate replacement ratio of 30%. All the prototypes were fabricated from an ASTM-A36 steel grade with nominal yielding and ultimate stresses of 250 and 430 MPa, respectively.

Tuper ® fabricators utilised a high-frequency induction welding to produce the tubes from the strip fed into rolls which formed the strip into a cylindrical shape. The mean values of the RCA replacement ratio and the measured geometric sizes of the steel and composite columns, including outer diameter (D), thickness (t), member length (L), steel and concrete areas (A_s and A_c), and the characteristic value of the cylinder compressive strength of concrete (f_{ck}), are presented in Table 1.

Table 1 – Geometrical properties mean values of the specimens – NACFST and RACFST.

Prototype	r [%]	D [mm]	t [mm]	D/t	L [mm]	L/D	A_c [mm^2]	A_s [mm^2]	A_s/A_c	f_{ck} [MPa]
S1	-	178.0	6.56	27.13	448.0	2.52	-	3420.28	-	-
S2										
S3	-	153.0	6.56	23.32	553.0	3.61	-	2913.57	-	-
S4										
C1-178-40-C00	0	178.0	6.55	27.16	548.33	3.08	21354.82	3529.73	0.17	31.43
C2-178-40-C00										
C3-178-40-C00										
C4-178-40-R30	30	178.0	6.57	27.10	560.00	3.15	21347.92	3536.63	0.17	35.13
C5-178-40-R30										
C6-178-40-R30										
C7-178-30-C00	0	178.0	6.56	27.15	558.67	3.14	21353.10	3531.45	0.17	24.26
C8-178-30-C00										
C9-178-30-C00										
C10-153-30-C00	0	153.0	6.56	23.34	451.00	2.95	15369.63	3015.76	0.20	29.51
C11-153-30-C00										
C12-178-30-R30	30	178.0	6.56	27.12	548.33	3.08	21349.64	3534.91	0.17	29.85
C13-178-30-R30										
C14-178-30-R30										
C15-153-30-R30	30	153.0	6.56	23.32	449.67	2.94	15367.43	3017.96	0.20	29.85
C16-153-30-R30										
C17-153-30-R30										
C18-178-30-R50	50	178.0	6.55	27.16	544.33	3.06	21354.82	3529.73	0.17	27.26
C19-178-30-R50										
C20-178-30-R50										
C21-153-30-R50	50	153.0	6.57	23.30	452.33	2.95	15364.50	3020.89	0.20	27.26
C22-153-30-R50										
C23-153-30-R50										

2.2 Material characterisation

The physical properties such as Young's Modulus (E), proof stress at 0.2% (f_y) and ultimate stress (f_u) for the steel cross-sections were obtained from the curved tensile coupon tests following Huang and Young [43] recommendations. As reported by the authors, the cross-sectional area is difficult to be accurately measured. Uniform tensile stress is not easily applied to the coupon specimen during testing due to their curved geometries. The curved coupons cannot be gripped by flat surface clamps due to their curved surfaces, therefore, two holes drilled at both ends of the coupons were drilled as shown in Figure 2. The tensile force was applied by two pins passing through the holes, which is in line with the centroid of the cross-section, to avoid bending stresses in the coupons. Six coupons were extracted from each cross-section as shown in Figure 3. The main material properties were obtained from the stress-strain curves presented in Figure 3 and reported in Table 2, in which E is the Young's Modulus, f_y and ε_y are the 0.2% proof stress and the corresponding strain at 0.2% proof stress, f_u and ε_u are ultimate stress and the corresponding strain at the ultimate stress.

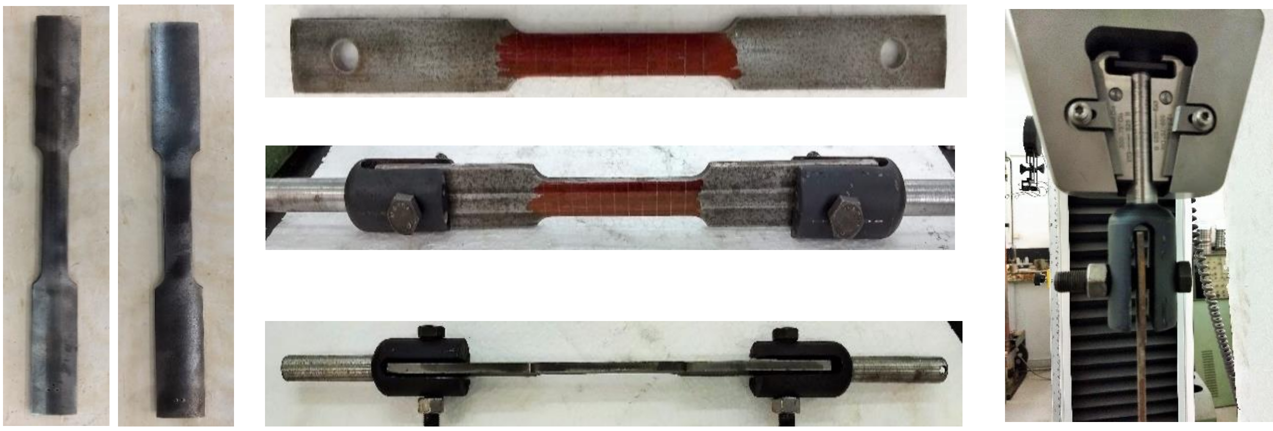

a) CP1 and CP2 before drilling

b) special device for curved coupon tests

c) device details

Figure 2. Preparation of tension test coupons.

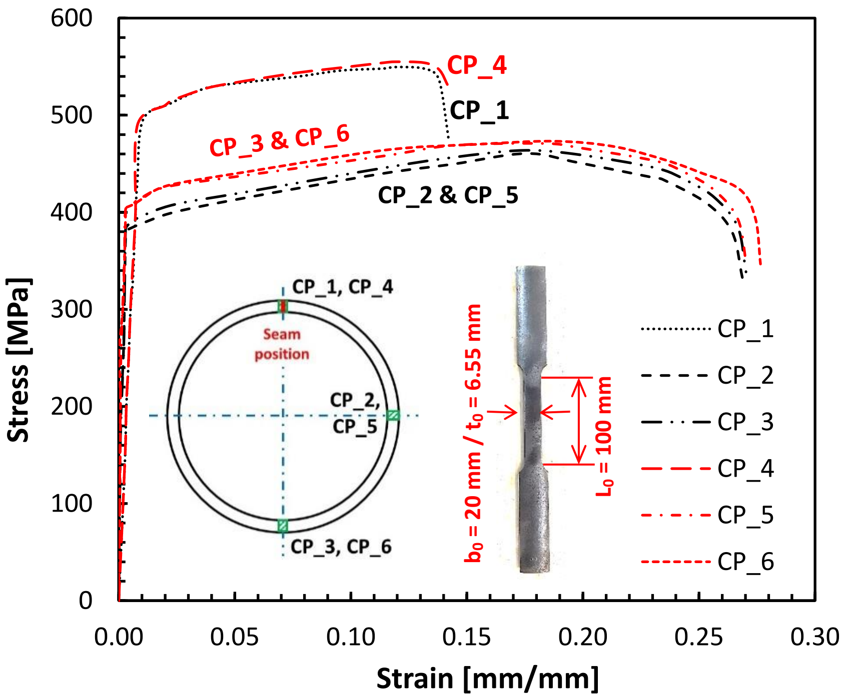

Figure 3. Coupon tests stress versus strain curves.

Table 2 – Steel physical properties.

Specimen	Tube diameter	E_{steel}	f_y	ε_y	f_u	ε_u
	(mm)	(GPa)	(MPa)	(mm/mm)	(MPa)	(mm/mm)
CP1	177.80	208.67	512.21	0.00224	569.77	0.1189
CP2	177.80	209.56	402.91	0.00295	470.84	0.1842
CP3	177.80	203.46	404.61	0.00301	473.20	0.1876
CP4	152.40	201.15	515.18	0.00228	555.65	0.1140
CP5	152.40	204.31	382.26	0.00293	460.53	0.1740
CP6	152.40	202.30	379.50	0.00299	463.74	0.1755

The concrete compressive cylinder strength was selected considering the universal test machine maximum load-carrying capacity and two expected values of f_{cm} (mean value of the measured cylinder compressive strength of concrete) at 28 days, i.e., 35 MPa and 45 MPa were chosen. These values correspond to approximately f_{ck} (characteristic value of the cylinder compressive strength of concrete) of 30 MPa and 40 MPa, respectively, with a standard deviation of 4 following the ABNT NBR 12655 design standard [44]. The RCA was produced through the crushing of concrete elements from a previous experimental campaign [45] of push-out tests, which had an average compressive cylinder strength of 41 MPa, as shown in Figure 4(a).

For the investigation performed herein, the traceability of the RCA origin is crucial to guarantee the reliability of the tests. The blocks from the push-out tests were fragmented in small parts, as presented in Figure 4(b), before introduced in the rubble recycler machine, Figure 4(c). they were divided into three different particle sizes - Figure 4(f) - for further use in the particle size distribution using the sieving method. The characterisation of the fine and coarse aggregates was performed according to ABNT NBR 7211 [46] and involved two samples for each. The adopted sand based on fineness modulus in the acceptable zone ranging from 2.9 to 3.5 and a single-sized coarse aggregate with a nominal size up to 9.5 mm were used to produce the recycled and natural aggregate concretes.


a) concrete blocks – push-out tests


b) concrete block preliminary fragmentation

c) rubble recycler machine


d) crushed recycled aggregate


e) particle size separation


f) characterised the recycled coarse aggregate

Figure 4. Recycled coarse aggregate preparation and characterisation.

The actual particle size distribution of each fine and coarse aggregates was measured using the sieving method given in [46]. The obtained percentages passing by mass for each sieve sizes of 1.18 mm, 2.36 mm, 4.75 mm, 6.30 mm, 9.52 mm and 12.5 mm are presented in Table 3 and Table 4, respectively, for fine and coarse aggregates. The grading curves of recycled coarse aggregate (RCA) are shown in Figure 5, where it can be observed which the obtained values are in accordance with the ABNT NBR 7211 [46] requirements for both adopted samples.

The test specimens were cast in five series using a similar concrete mix design presented in Table 5. The first and third series concerning tests C1 to C3 and C7 to C11 only contained natural coarse aggregate (NCA), whereas the second (C4 to C6), fourth (C12 to C17) and fifth series (C18 to C23) had 30%, 30% and 50% of the NCA replaced with the same amount of recycled coarse aggregate (RCA). It is noted that the recycled aggregates had, as expected, a significantly greater water absorption capacity compared with the natural coarse aggregates. Following the recommendations of other researchers who used RAC [47], [48], the recycled aggregates were treated before casting by first sieving to ensure that the particles were the same size as the natural coarse aggregates. After that, water was added just before casting and mixing it in the saturated condition to compensate for the higher water absorption properties.

Table 3 - Fine aggregates grain composition

Diameter of the sieve's mesh (mm)	Withheld material (g)		Withheld percentage (%)		Accumulated material (%)	
	Sample 1	Sample 2	Sample 1	Sample 2	Sample 1	Sample 2
12.50	0	0	0	0	0	0
9.52	0	0	0	0	0	0
6.30	0	0	0	0	0	0
4.75	0	0	0	0	0	0
2.36	12.44	14.65	1.24	1.47	1.24	1.47
1.18	261.25	278.84	26.13	27.88	27.37	29.35
0.60	503.29	505.29	50.33	50.53	77.70	79.88
0.30	138.55	133.80	13.86	13.38	91.55	93.26
0.15	55.19	48.95	5.52	4.90	97.07	98.15
Pallet	29.28	18.47	2.93	1.85	100.00	100.00
Fineness modulus					2.99	
Maximum size (mm)					2.36	

Table 4 - coarse aggregates grain composition

Diameter of the sieve's mesh (mm)	Withheld material (g)		Withheld percentage (%)		Accumulated material (%)	
	Sample 1	Sample 2	Sample 1	Sample 2	Sample 1	Sample 2
12.50	0	0	0	0	0	0
9.52	88.60	84.40	4.43	4.22	4.43	4.22
6.30	1138.90	1029.86	59.95	51.50	61.40	55.71
4.75	472.20	516.76	23.61	25.84	84.99	81.55
2.36	148.78	210.25	7.44	10.51	92.42	92.06
1.18	51.92	52.05	2.60	2.60	95.02	94.67
0.60	0	0	0	0	95.02	94.67
0.30	0	0	0	0	95.02	94.67
0.15	0	0	0	0	95.02	94.67
Pallet	99.60	106.66	4.98	5.33	100.00	100.00
Fineness modulus					5.86	
Maximum size (mm)					9.52	

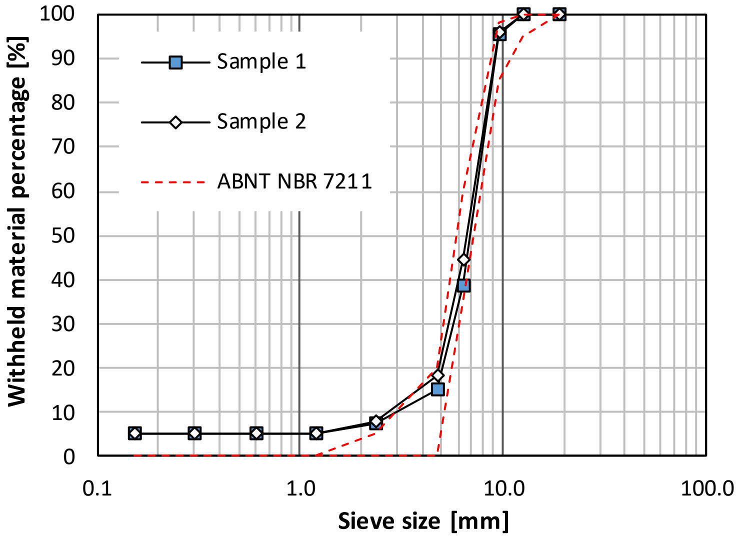

Figure 5. Recycled coarse aggregate grading curves.

A superplasticiser was included in both concrete mixes to make it more workable. The quantity was selected as approximately 0.15% of the cement weight. The RAC (recycled coarse aggregate concrete) reached a compressive cylinder strength greater than the standard coarse aggregate concrete (NAC) as summarised in Table 6. This was determined by conducting compressive tests on cylindrical samples (CS) from each batch of concrete, as shown in Figure 6, on the same day that the corresponding columns were tested. Additionally, this fact may be justified because the RAC was produced from a well characterised concrete taken from the push-out tests with a cylinder compressive strength of 41 MPa.

a) recycled aggregate concrete failure mode

c) conventional concrete failure mode

Figure 6. Failure modes of the RAC and NAC cylinder compressive tests.

Table 5 - Concrete's mix proportions.

Prototype	Total volume (concrete + RACFST + loss of 5%)	Cement CPII-E-32	Sand	NCA	RCA	Water	Water-to-cement ratio	Additive
	(m^3)	(kg)	(kg)	(kg)	(kg)	(kg)	(a/c)	(l)
C1-178-40-C00	0.0569	22.02	49.50	54.00	0	10.58	0.48	0.279
C2-178-40-C00								
C3-178-40-C00								
C4-178-40-R30	0.0569	22.02	49.50	37.80	16.20	10.58	0.54	0.279
C5-178-40-R30								
C6-178-40-R30								
C7-178-30-C00	0.0713	24.53	63.53	66.45	0	13.26	0.54	0.314
C8-178-30-C00								
C9-178-30-C00								
C10-153-30-C00								
C11-153-30-C00								
C12-178-30-R30	0.0786	27.04	70.03	51.28	21.98	14.62	0.54	0.346
C13-178-30-R30								
C14-178-30-R30								
C15-153-30-R30								
C16-153-30-R30								
C17-153-30-R30								
C18-178-30-R50	0.0786	27.04	70.03	36.63	36.63	14.62	0.54	0.346
C19-178-30-R50								
C20-178-30-R50								
C21-153-30-R50								
C22-153-30-R50								
C23-153-30-R50								

Table 6 – Concrete mechanical properties.

Concrete type and Tests ID	r (%)	Specimen ID	f_{ck} [MPa]		Ec_s [GPa]		
			Expected	28 days	NBR 8800	EC4	28 days
NCA_C40 C1 to C3	0	CS1	38.40	28.90	26.26	34.18	23.37
		CS2	38.40	33.95	28.87	35.52	25.41
RCA_C30 C4 to C6	30	CS3	38.40	36.27	30.04	36.09	25.53
		CS4	38.40	33.97	28.88	35.52	25.13
NCA_C30 C7 to C9	0	CS5	28.40	23.27	23.18	32.52	20.63
		CS6	28.40	25.24	24.28	33.12	20.88
NCA_C30 C10 and C11	0	CS7	28.40	29.05	26.34	34.22	23.18
		CS8	28.40	29.97	26.82	34.47	22.80
RCA_C30 C12 to C17	30	CS9	28.40	29.20	26.42	34.26	21.93
		CS10	28.40	30.50	27.10	34.61	23.03
RCA_C30 C18 to C23	50	CS11	28.40	26.75	25.11	33.57	21.09
		CS12	28.40	27.77	25.66	33.86	21.30

For the NACFST and RACFST columns investigated in this work, the steel contribution ratio $\delta = \left(Af_y/N_{pl,Rd}\right)$ reached a mean value of 0.65 evaluated with the real mechanical properties of steel and concrete materials. This value is in range within the EC4 [39] requirements of $0.2 \leq \delta \leq 0.9$ for composite columns.

2.3 Test layout and instrumentation

The instrumentation used in the tests aimed to measure the column displacements and strains. The displacements were acquired with six LVDT (Linear Variable Differential Transducer) as shown in Figure 7(a). Two displacement transducers measured the column axial displacement in the load direction (V1 and V2) while four were positioned in the quadrants of the cross-section at the column mid-height (V3, V6 to V8) were used to acquire the column lateral displacements. Four strain gauges (S0 to S3) acquired the column load direction strains in the column cross-section quadrants.

Reinforcement radial stiffeners were used to avoid local buckling (“elephant foot”) at the column ends as suggested by Wang et al. [49] as shown in Figure 7(b). Two carbon steel radial stiffeners were used at both ends with a thickness of 7 mm and a length of 50 mm. The radial stiffeners diameters were adjusted to fit perfectly with the column tube outer diameter avoiding undesirable gaps. Steel plates, 30 mm thick, were positioned at the column ends to better distribute the compression loads. All tests were performed under monotonic displacement control at a constant rate of 0.003mm/s using a 3000kN capacity servo-controlled hydraulic testing machine. This procedure allows the test to be continued beyond the ultimate load and the post-ultimate behaviour to be recorded. A general layout of the tests is shown in Figure 7(c).

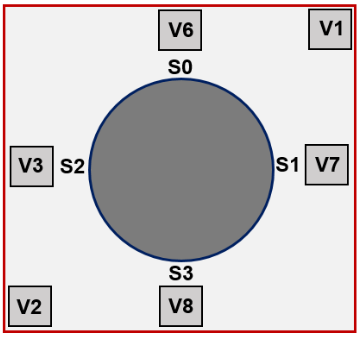

a) top view of the LVDT's and strain gauge's location

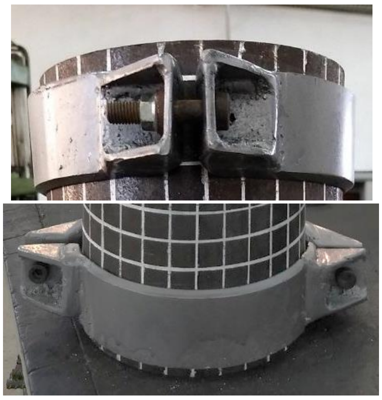

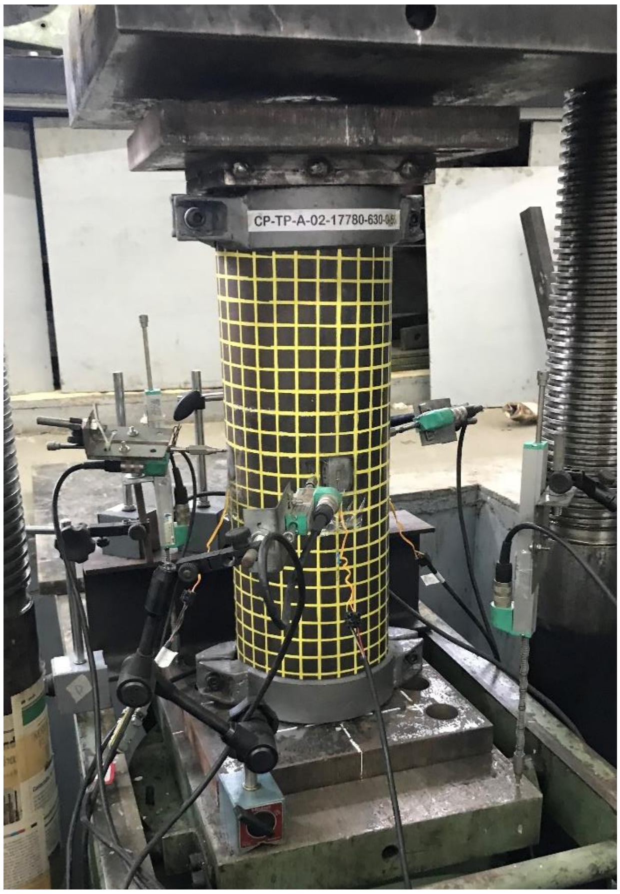

b) radial stiffeners c) experimental layout

Figure 7. Experimental layout and instrumentation.

3. Experimental results

3.1 General

The overall response of the NACFST and RACFST columns was observed during the tests. The load versus axial displacements curves and the load versus axial strain curves for each prototype were assessed. The axial strains were determined as the average of the measured values obtained from four strain gauges positioned at the column mid-height, as reported in the last section. Additionally, the observed failure modes are also reported herein. With these results in hand, it was possible to investigate the influence of different replacement percentages of recycled coarse aggregate (RCA) of 0%, 30% and 50% in the composite column's behaviour. Additionally, the influence of the concrete compressive strength was also studied.

3.2 Failure modes and deformed shapes

For steel columns prototypes S1 to S4, the observed failure mode was characterised by a single outward local buckling of the steel tube, as can be observed in Figure 8. For the composite columns, a combination of two or three outward local buckling was detected due to the presence of the infill concrete that inhibited inward deformations and confirmed the ductile response of the composite cross-sections as shown in Figure 9. An infill concrete crushing was also observed in the regions where the local buckling of the steel tubes occurred, as presented in Figure 10 and Figure 11, where the prototypes C1-178-40-C00 for NACFST and C18-178-30-R50 for RACFST columns were cut through in their centroid. The seam of the tubes may also be observed in Figure 10 and Figure 11 as well. The concrete crushing may indeed have triggered the local buckling failures, as reported by Wang et al. [49].

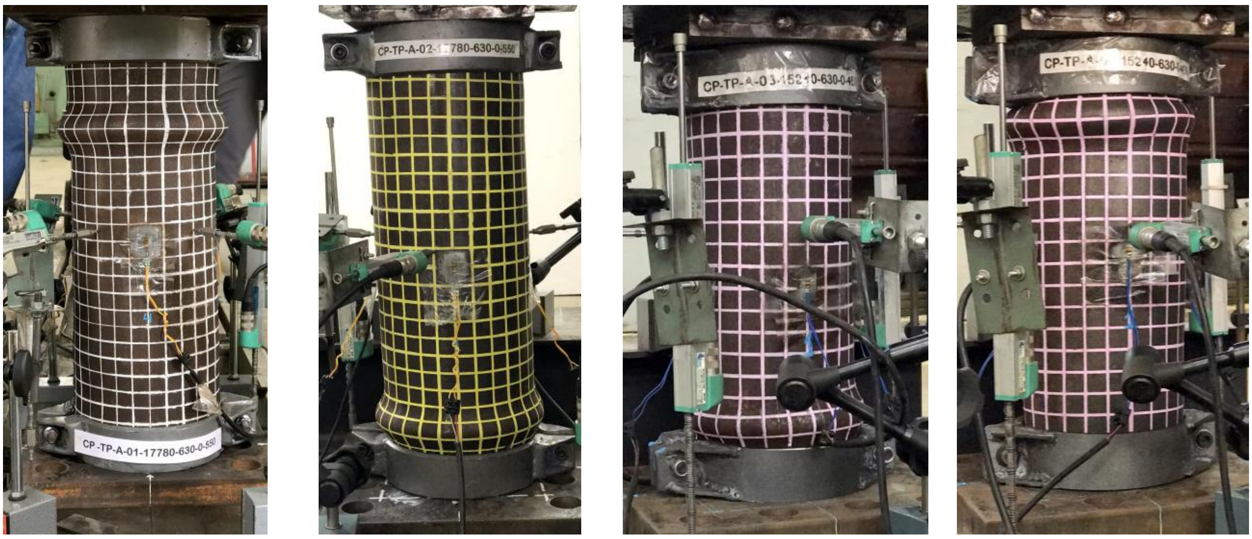

S1 S2 S3 S4

Figure 8. Steel columns deformed configurations.

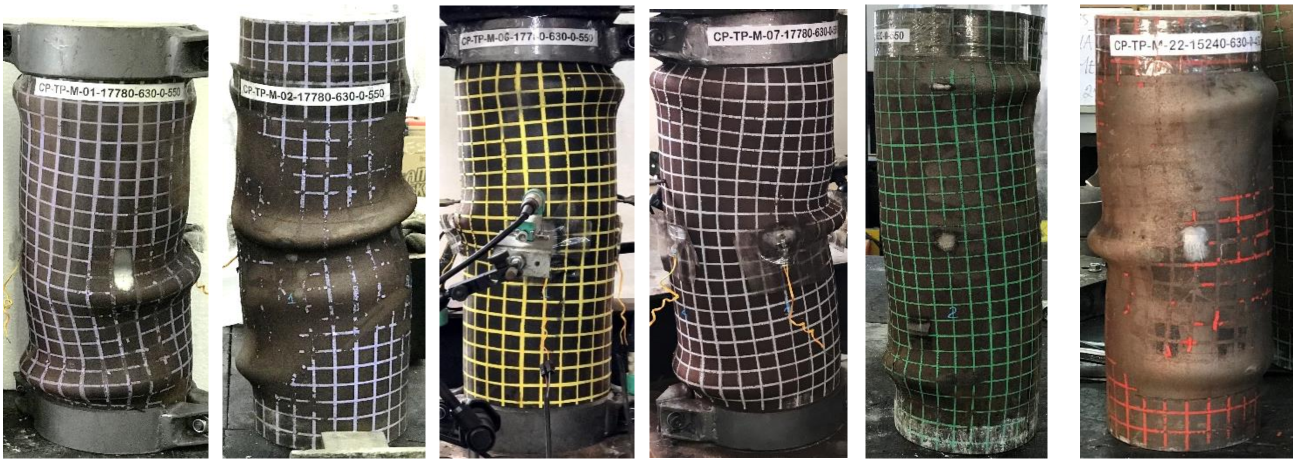

Figure 9. Composite columns deformed configurations– steel tube outward local buckling.

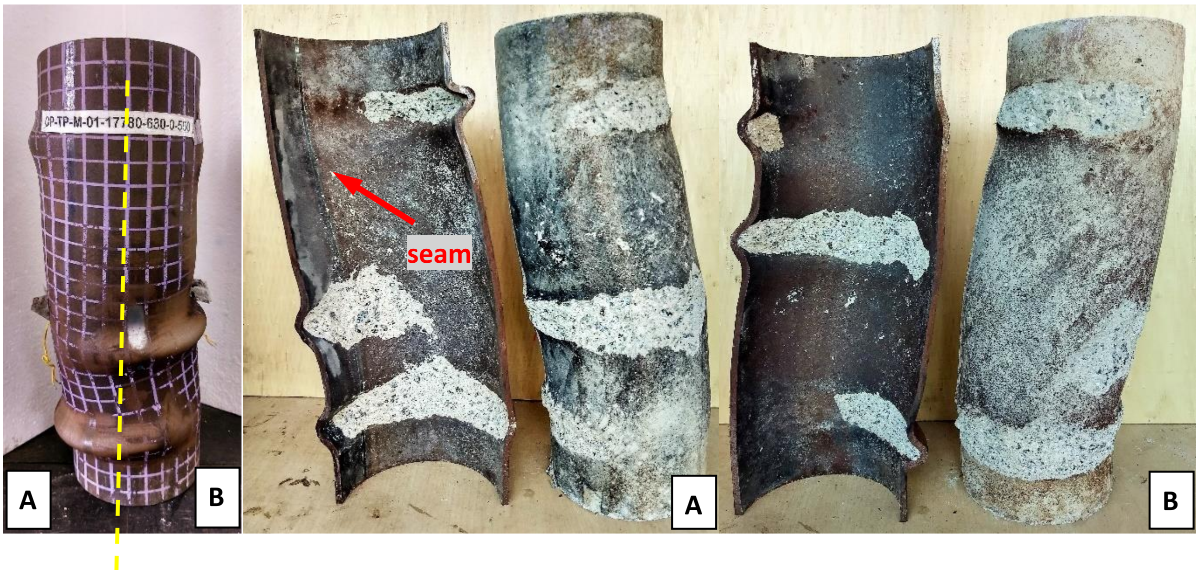

Figure 10. Composite column C1-178-40-C00 – NACFST - diameter of 177.80 mm and r = 0%.

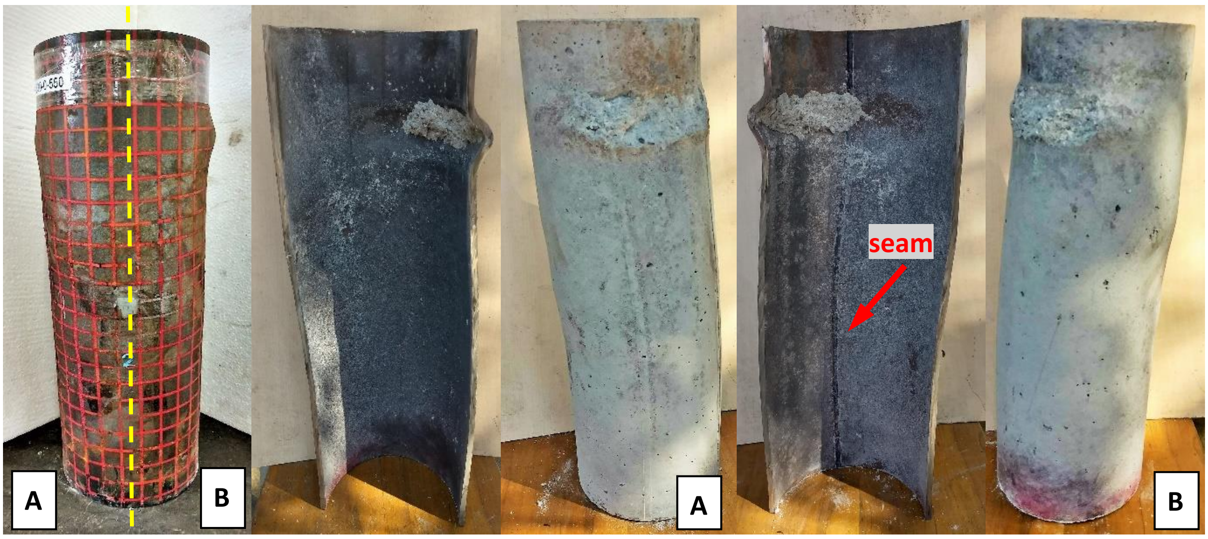

Figure 11. Composite column C18-178-30-R50 - RACFST - diameter of 177.80 mm and r = 50%.

3.3 Influence of the recycled aggregate replacement ratio – r (%) and concrete compressive strength

The load versus axial displacements curves and the load versus axial strain curves for the tests with 178 mm diameter and a concrete compressive cylinder strength of 30 MPa are presented in Figure 12. The ultimate experimental loads (P_{exp}) are summarised in Table 7 for NACFST and RACFST stub columns where the confinement factor ξ is defined as $f_y A_s / f_c A_c$. Additionally, the two steel stub column tests are also reported to identify the resistance increase when using composite columns. It is worth mentioning herein that the S1 test was used to calibrate the load application system. The ultimate loads for S1 and S2 tests were 1822.01kN and 1717.63kN, respectively, corresponding to a difference of approximately 9.4%.

Table 7 – Experimental and design standards ultimate load – NACFST and RACFST.

Prototype	r [%]	D [mm]	t [mm]	ξ	P_{EXP} [kN]	P_{EXP}- [kN] mean values	P_{EC4} or $P_{AS/NZS}$ [kN]	P_{NBR} or P_{AISC} [kN]	P_{exp}/P_{EC4} or $P_{exp}/P_{AS/NZS}$	P_{exp}/P_{NBR} or P_{exp}/P_{AISC}
C1-178-40-C00	0	178.0	6.55	2.12	2753.1		2440.3	1879.9	1.13	1.46
C2-178-40-C00	0	178.0	6.56	2.13	2796.7	2780.8	2441.8	1881.9	1.15	1.49
C3-178-40-C00	0	178.0	6.55	2.12	2792.6		2438.8	1879.9	1.15	1.49
C4-178-40-R30	30	178.0	6.56	1.90	2901.6		2492.0	1935.5	1.16	1.50
C5-178-40-R30	30	178.0	6.57	1.91	2896.3	2877.0	2493.1	1937.4	1.16	1.49
C6-178-40-R30	30	178.0	6.57	1.91	2833.1		2492.8	1937.4	1.14	1.46
C7-178-30-C00	0	178.0	6.55	2.75	2675.3		2331.9	1776.1	1.15	1.51
C8-178-30-C00	0	178.0	6.56	2.75	2636.1	2662.2	2335.6	1778.1	1.13	1.48
C9-178-30-C00	0	178.0	6.56	2.75	2675.1		2335.9	1778.1	1.15	1.50
C10-153-30-C00	0	153.0	6.55	2.53	2413.7	2405.4	1901.1	1455.7	1.27	1.66
C11-153-30-C00	0	153.0	6.56	2.53	2397.1		1903.8	1457.3	1.26	1.64
C12-178-30-R30	30	178.0	6.57	2.24	2701.6		2421.7	1861.0	1.12	1.45
C13-178-30-R30	30	178.0	6.56	2.24	2746.9	2731.8	2419.4	1859.0	1.14	1.48
C14-178-30-R30	30	178.0	6.56	2.24	2746.9		2419.4	1859.0	1.14	1.48
C15-153-30-R30	30	153.0	6.57	2.51	2119.6		1909.7	1462.3	1.11	1.45
C16-153-30-R30	30	153.0	6.56	2.51	2390.7	2245.3	1907.0	1460.8	1.25	1.64
C17-153-30-R30	30	153.0	6.55	2.50	2225.6		1905.6	1459.2	1.17	1.53
C18-178-30-R50	50	178.0	6.55	2.45	2771.3		2378.1	1819.5	1.17	1.52
C19-178-30-R50	50	178.0	6.55	2.45	2714.8	2693.8	2378.5	1819.5	1.14	1.49
C20-178-30-R50	50	178.0	6.56	2.45	2595.3		2388.7	1821.5	1.09	1.42
C21-153-30-R50	50	153.0	6.57	2.75	2283.2		1881.9	1435.3	1.21	1.59
C22-153-30-R50	50	153.0	6.56	2.74	2247.7	2237.0	1879.8	1433.8	1.20	1.57
C23-153-30-R50	50	153.0	6.57	2.75	2180.2		1881.5	1435.3	1.16	1.52
								Mean	1.16	1.51
								SD	0.05	0.06

	CoV	0.04	0.04

On the other hand, when the ultimate loads of S3 and S4 tests with 153 mm diameter are compared in Figure 13, the respective values were 1449.18 kN and 1464.32 kN showing a good agreement and that the system calibration had been correctly performed. The mean experimental ultimate loads for C7 to C9 (r=0%), C12 to C14 (r=30%) and C18 to C20 (r=50%) tests were 2662.2kN, 2731.8kN and 2693.8kN, respectively. Analysing these values, it is possible to verify that using the recycled aggregate concrete provided column's resistances with similar maximum values. Additionally, it is important to mention that this behaviour was also observed because the concrete compressive cylinder strength in the tests C12 to C14 (r=30%) and C18 to C20 (r=50%) equal to 29.85 MPa and 27.26 MPa, respectively, that were slightly greater than the compressive cylinder strength of the tests C7 to C9 (r=0%) equal to 24.26 MPa. On the other hand, a significant number of the NACFST columns presented a more ductile behaviour when compared to the RACFST columns. This trend can be explained due to the use of recycled aggregate concrete extracted from concrete blocks of a previous experimental campaign [45], which had an average compressive cylinder strength of 41 MPa, higher than the obtained strengths of the concrete considered in the composite columns.

Similar behaviour was observed in Figure 13, where the results for the C1 to C3 (r=0% and C4 to C6 (r=30%) tests with a 178mm diameter and a concrete compressive strength of 40 MPa are presented. In these tests, the mean ultimate loads were 2780.8 kN and 2877.0 kN, respectively. Additionally, observing the load versus strains curves in Figure 13 (b) for these tests, the RACFST columns presented larger strains at the same load level when compared to the NACFST columns.

When the composite columns with 153mm diameter and an expected concrete compressive cylinder strength of 30 MPa, C10 and C11 (r=0%), C15 to C17 (r=30%) and C21 to C23 (r=50%), are compared in Figure 14, it may be observed that the NACFST columns presented ultimate loads higher than the RACFST columns. The obtained mean values were 2405.4 kN, 2245.3 kN and 2237.0 kN for r=0%, r=30% and r=50%, respectively. Despite these results, the decrease in the RACFST columns resistances was approximately 7%, highlighting that the use of the recycled coarse aggregate only slightly influenced the response of the column.

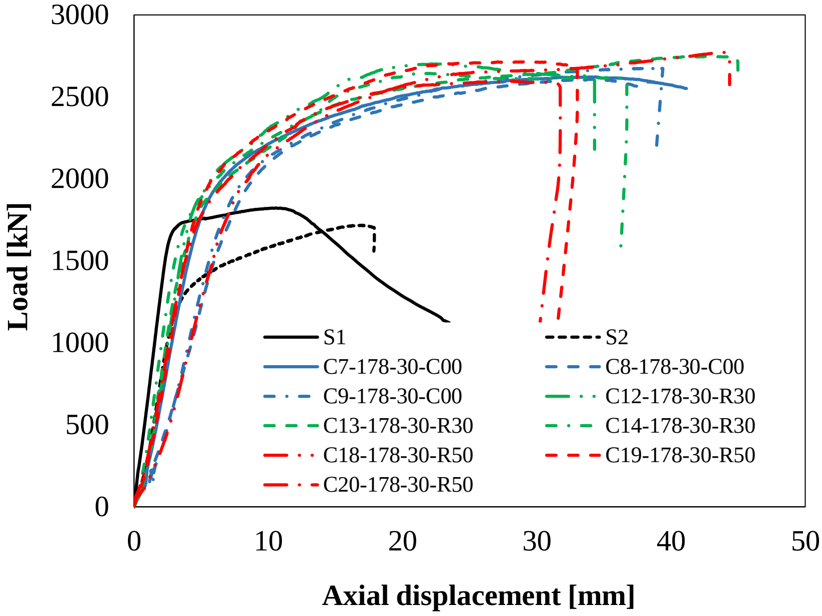

a)

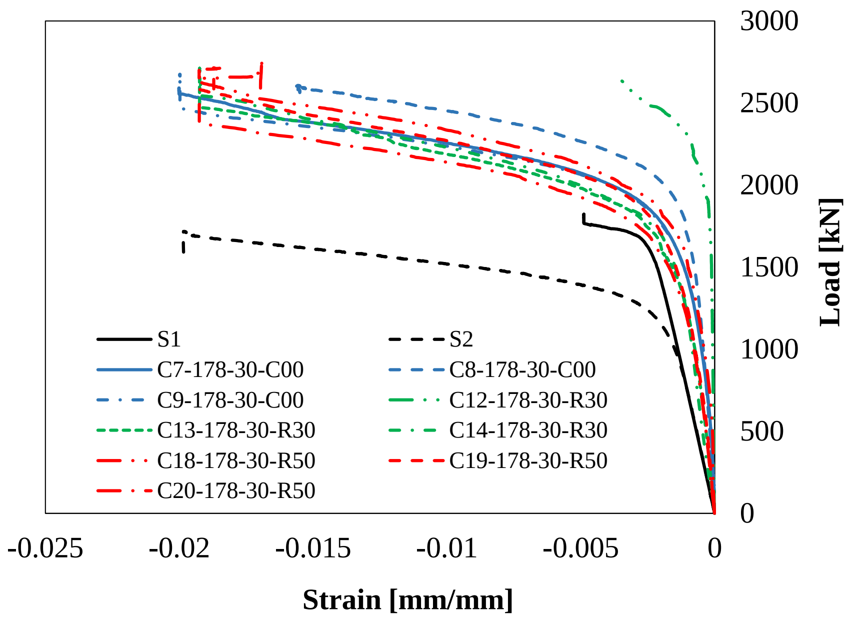

b)

Figure 12. Composite columns with 30MPa and a 178.0 mm diameter.

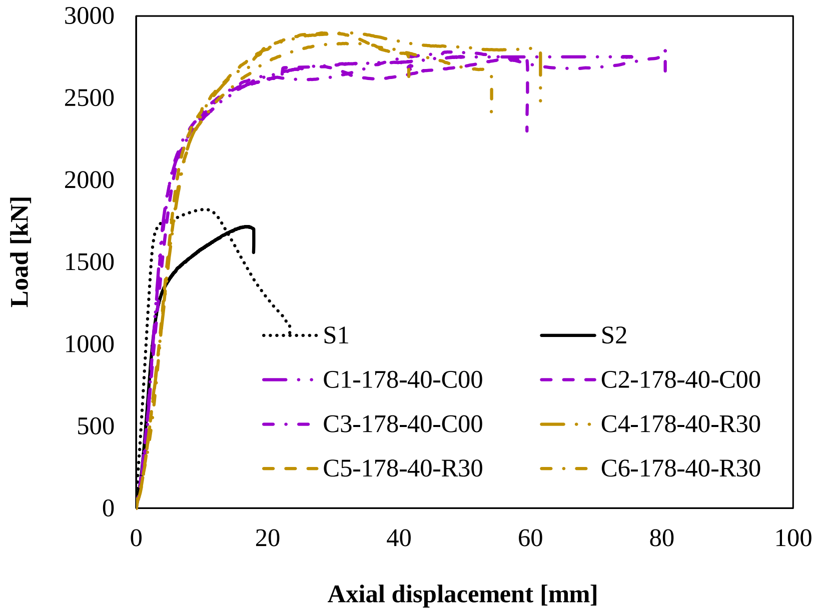

a)

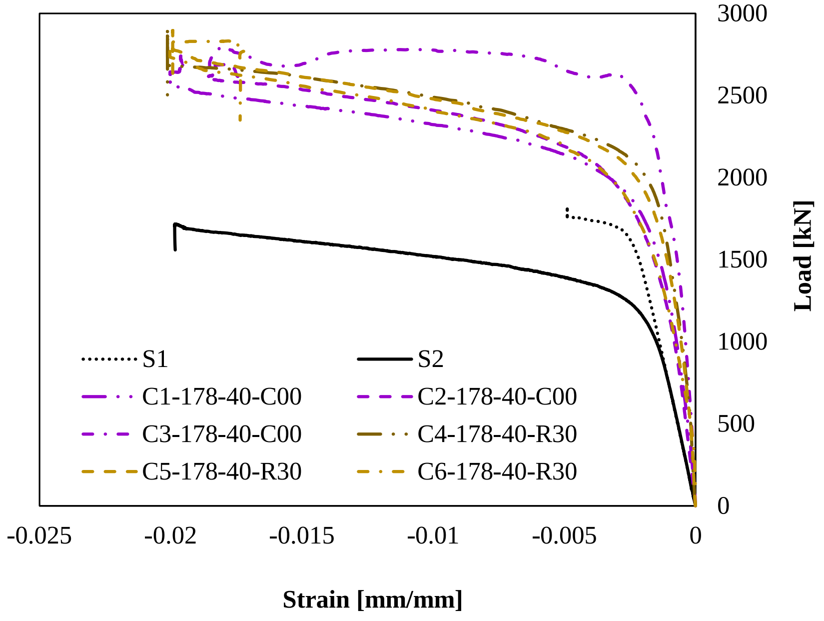

b)

Figure 13. Composite columns with 40MPa and a 178.0 mm diameter.

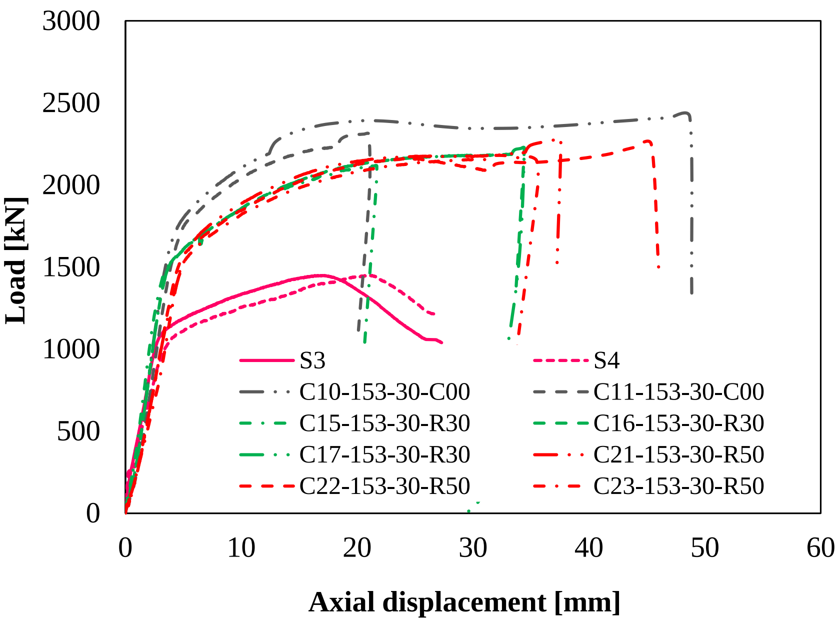

a)

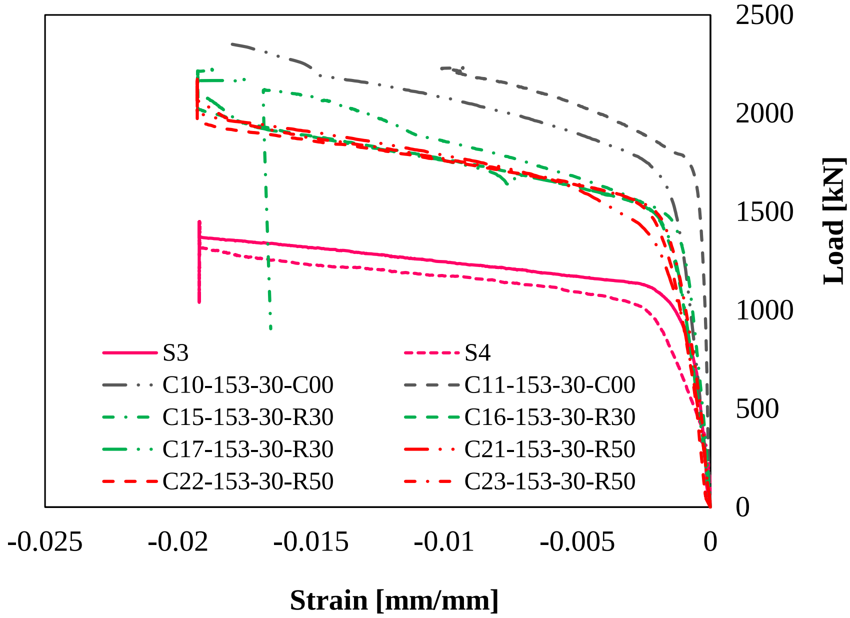

b)

Figure 14. Composite columns with 30 MPa and a 153.0 mm diameter.

Aiming to investigate the influence of the concrete compressive strength in the composite column’s behaviour, two sets of tests can be assessed, i.e., first C1 to C3 and C7 to C9 and second, C4 to C6 and C12 to C14. These tests correspond to cases of prototypes with 178 mm diameter and recycled aggregate replacement ratio of 0% and 30%, respectively. For the first set presented in Figure 15, the mean values of the ultimate loads for the tests C1 to C3 and C7 to C9 were 2780.8 kN and 2662.2 kN, corresponding to the concrete compressive strengths of 31.4 MPa and 24.3 MPa. The mean ultimate load decrease was 4.5% approximately while the reduction in the concrete compressive strength was 29.2%.

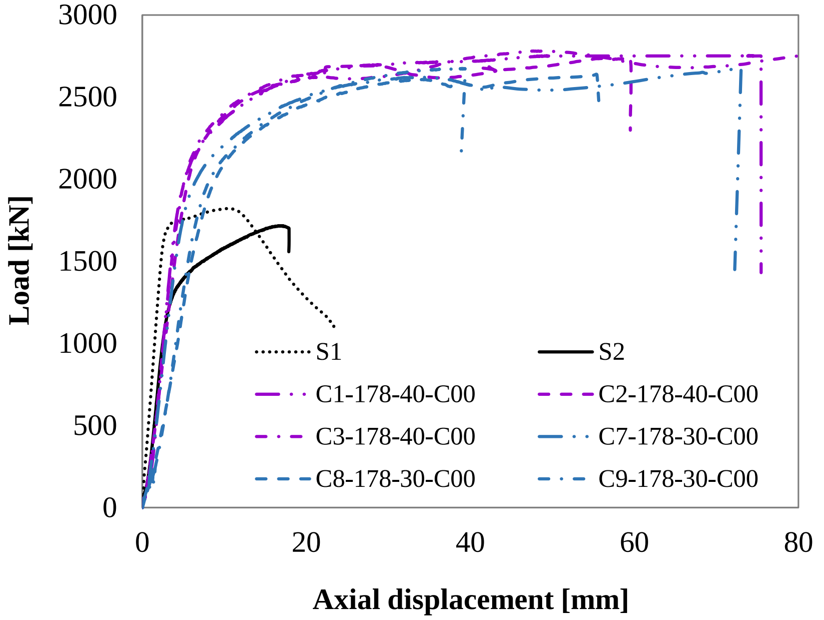

a) r = 0% (first set)

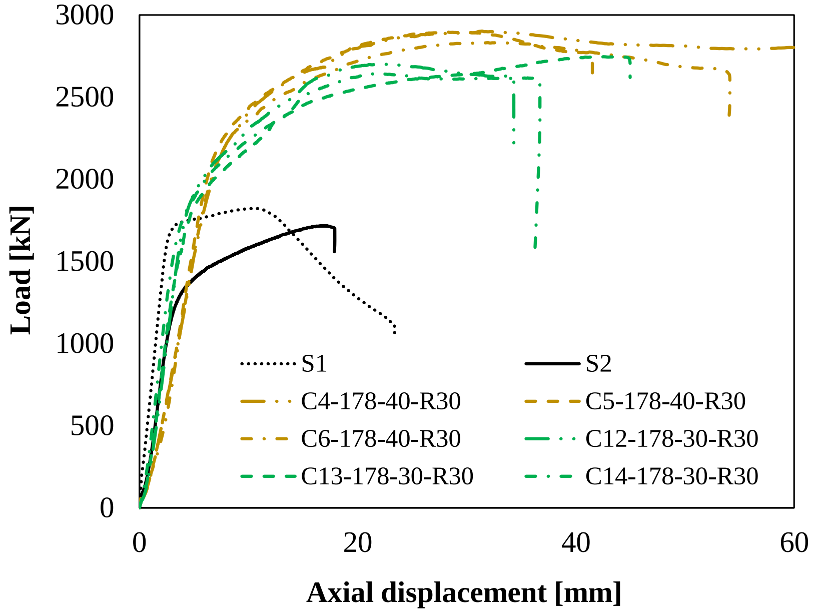

b) r = 30% (second set)

Figure 15. Concrete compressive strength influence – 178.0 mm diameter.

For the second set of tests, C4 to C6 and C12 to C14, the mean ultimate loads were 2877.0 kN and 2731.8 kN respectively corresponding to a decrease in resistance of approximately 5.3%, while the reduction in the concrete compressive cylinder strength was 17.8 %, i.e., 35.1 MPa to 29.8 MPa. With these results in hand, it is possible to observe that the composite column's resistances increase is not only dependent on the concrete compressive strength but also depends on the steel and concrete compressive strength f_y/f_c ratio, which characterises the confinement effect. The confinement factor $\xi = f_y A_s / f_c A_c$ proved to be an important variable to be considered for composite columns. For the first set, a mean confinement factor of 2.12 can be calculated for tests C1 to C3 compared to 2.75 for the tests C7 to C9, corresponding to a variation of 29.2%. This value for C4 to C6 tests was 1.90 compared to 2.24 for the C12 to C14 tests, characterising a difference of 17.6%.

Additionally, Figure 16 presents the contribution of each material, steel $(A_s f_y)$ and concrete $(A_c f_{ck})$ in the composite column's resistances where the confinement effects can be observed. The mean contribution for each set of equal tests are also presented. The major increase in the composite column's resistance due to confinement effects was achieved for the tests C10, C11 and C16, corresponding to the large values of t/D = 0.043 and ξ = 2.5. In these tests, the mean confinement contribution was 33% of the ultimate column resistance.

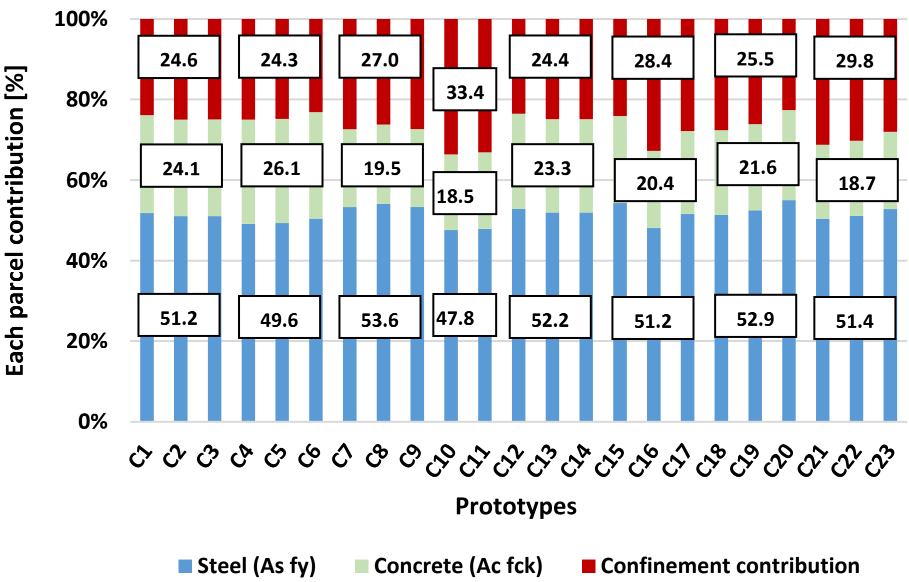

Figure 16. Percentage contribution of individual parcels in the composite column's resistances.

4. Design codes assessment

4.1 Generalities

It is widely known that there are still no design codes for carbon-steel recycled aggregate concrete composite structures. The current design codes including ABNT NBR 8800 [35] , ABNT NBR 16239 [36], AISC 360-16 [38], Eurocode 4 [39] and Australian/New Zealand standard AS/NZS 2327 [40] can only be used for circular natural aggregate concrete-filled carbon steel tubular (NACFST) columns. Despite these limitations, these codes were utilised to verify their applicability to circular RACFST columns. Initially, the specified design rules for circular NACFCST columns are presented based on non-factored compression resistances of the composite circular columns. These predictions were calculated using the RAC, and NAC measured material strengths and carbon steel proof stress at a 0.2% strain. The applicability of each design code was checked by comparing the test failure loads P_{exp} against non-factored compression resistance P_{codes} in terms of the P_{exp}/P_{codes} mean ratio and their corresponding coefficient of variation (CoV), as presented in Table 7.

4.2 American AISC 360–16 (AISC), Brazilian NBR16239 and NBR8800 (ABNT) specifications

The compressive plastic resistance of a circular NACFST column P_{ABNT} or P_{AISC} as specified in the Brazilian ABNT NBR8800 [35], ABNT NBR 16239 [36] and American AISC 360–16 [38], is calculated by adding the plastic resistances of its components, i.e., the steel tube area A_s multiplied by the yield stress f_y plus the concrete area A_c multiplied by the concrete compressive cylinder strength f_{cd} using a factor of 0.95 instead of 0.85 to consider the confinement afforded by the steel tube as given by Eq. (1). The same procedure is adopted in ABNT NBR8800 [35] and ABNT NBR 16239 [36]. A slenderness limit of $D/t \leq 0.15\left(E/f_y\right)$ for concrete-filled composite members is defined in the Brazilian ABNT NBR8800 [35] and AISC 360–16 [38], beyond which the effects of local buckling need to be considered.

$$P_{AISC} = P_{ABNT} = A_s f_{yd} + 0,95 A_c f_{cd} \quad (1)$$

4.3 European code EN 1994-1-1 (EC4) and Australian/New Zealand AS/NZS 2327 standard specifications

Similarly, the European code EN 1994-1-1 [39] and Australian/New Zealand standard AS/NZS 2327 [40] consider that the plastic resistance to compression P_{EC4} and P_{AS} of a circular NACFCST column should be calculated by adding the plastic resistances of its components as presented in Eq. (2). The cross-sections plastic resistances can be used for circular NACFCST columns presenting member relative slenderness less than or equal to 0.5 and a limit for the cross-section slenderness $D/t = 90(235/f_{yd})$. The interaction between the steel tube and the concrete may be considered through two coefficients η_{ao} and η_{co}, calculated by Eqs. (3) and (4), respectively, that account for the confinement effects.

$$P_{EC4} = P_{AS} = \eta_{ao}(A_a \times f_{yd}) + \left(1 + \eta_{co}\frac{t}{D}\frac{f_y}{f_{ck}}\right)(A_c \times f_{cd}) \quad (2)$$

$$\eta_{ao} = 0.25(3 + 2\overline{\lambda}) \leq 1.0 \quad (3)$$

$$\eta_{co} = 4,9 - 18,5\overline{\lambda} + 17\overline{\lambda}^2 \geq 0 \quad (4)$$

where $\overline{\lambda}$ is the relative member slenderness, as defined in EC4 [34], it is worth mentioning that the buckling effective length factor was taken as 0.5 in the present study to reproduce the experiments fixed-ended boundary conditions.

5. Experimental results against design codes predictions

Figure 17 illustrates the ratio between experimental failure loads to the design predictions (P_{exp}/P_{codes}) ratios for all NACSFT and RACSFT columns. The design load predictions were evaluated using the measured geometrical and mechanical properties presented in Table 1 and Table 7. As aforementioned, the effective buckling length was considered equal to half of the column length presented in Table 1 as also reported by Wang et al. [49].

This comparison was made in terms of the design codes equations previously mentioned, i.e., ABNT NBR 8800 [35], AISC 360-16 [38], Eurocode 4 [39] and Australian/New Zealand standard AS/NZS 2327 [40]. According to Table 7 and, related to the ABNT NBR 8800 [35] and AISC 360-16 [38] recommendations, it could be observed that a large ratio was reached, showing the well-known conservatism of these codes since no confinement contribution is considered in the design equations. These values presented a mean value of 1.51, a standard deviation of 0.06 and a corresponding CoV of 0.04.

In contrast, when Eurocode 4 [39] and Australian/New Zealand standard AS/NZS 2327 [40] predictions are considered, a more consistent and economical design can be obtained corresponding to a mean ratio value of 1.16 with a CoV of 0.04. This is expected because these codes considered the concrete core confinement contribution. Based on these results, it could be concluded that the recommendations from these standards can be used to predict the ultimate capacity of NACSFT and RACSFT columns. At this point, it is important to stress that the Eurocode 4 [39] and Australian/New Zealand standard AS/NZS 2327 [40] led to more economical and consistent design predictions.

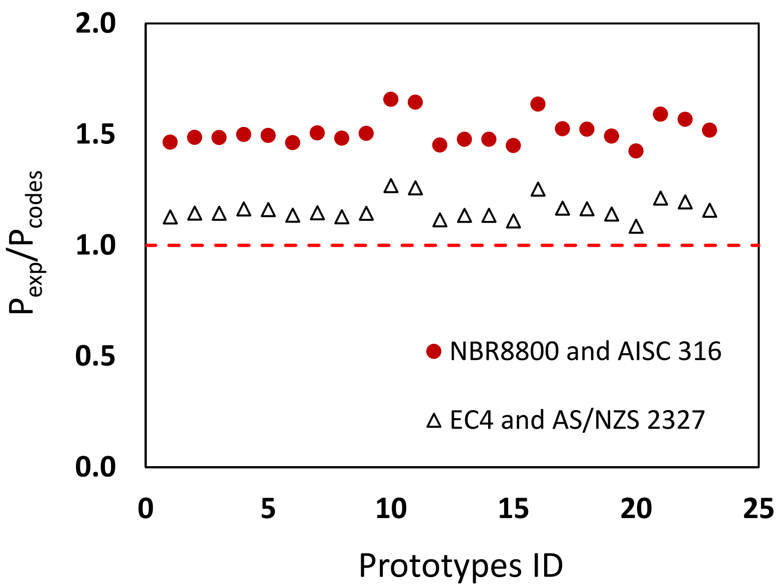

Figure 17. Concrete compressive strength influence – 178.0 mm diameter.

6. Conclusions

The present investigation was centred on an experimental campaign involving columns with different recycled coarse aggregate replacement percentages (RCA): 0%, 30% and 50%. The steel columns failure mode was characterised by a single outward steel tube local buckling while the composite columns reached an outward local buckling pattern and confirmed the composite cross-sections ductile response.

The mean experimental ultimate loads indicated that the recycled aggregate concrete usually provided column resistances similar to equivalent columns with standard concrete cores. Despite this fact, the NACFST columns presented a more ductile behaviour when compared to the RACFST columns. The influence of the concrete compressive strength over the composite column's behaviour was evidenced by comparing test results with concrete compressive cylinder mean strengths of 31.4 MPa and 24.3 MPa. It could be observed that the composite column's resistances increase is not only dependent on the concrete compressive strength but also depends on the steel and concrete compressive strength f_y/f_c ratio. The confinement factor proved to be an important variable to be considered in the response of the composite column.

Using ABNT NBR 8800 and AISC 360-16 recommendations, a large ratio (P_{exp}/P_{codes}) was observed, showing the well-known conservatism of these codes since no confinement contribution is considered in the design equations. On the other hand, when Eurocode 4 and Australian/New Zealand standard AS/NZS 2327 predictions are considered, a more consistent and economical design can be obtained since they considered the concrete core confinement contribution. These results indicated that all the recommendations from these standards could be safely used to predict the ultimate capacity of NACSFT and RACSFT columns.

7. Acknowledgements

The authors would like to thank CNPq (305143/2015-8; 306042/2013-4; 305026/2017-8) and FAPERJ (E-26/202.789/2017; E-26/010.101216/2018; E-26/202.924/2019 and E-26/202.532/2018) for the financial support to this research program.

REFERENCES

[1] S.A. Mirza, Parametric study of composite column strength variability. Journal of Constructional Steel Research, 2 (1989) 121-137.

[2] K. Konno, Y. Sato, T. Ueda, Mechanical property of recycled concrete under lateral confinement. Transactions of the Japan Concrete Institute, 20 (1997) 287-292.

[3] R.Q. Bridge, M.D. O' Shea, Behavior of thin-walled steel box sections with or without internal restraint. Journal of Constructional Steel Research, 77 (1998) 73-91.

[4] R.Q. Bridge, M.D. O' Shea, Design of circular thin-walled concrete filled steel tubes. Journal of Structural Engineering, ASCE, 126 (2000) 1295-1303.

[5] E. Ellobody, B. Young, D. Lam, Behaviour of normal and high strength concrete-filled compact steel tube circular stub columns. Journal of Constructional Steel Research, 62 (2006) 706-715.

[6] P. K. Gupta, S.M. Sarda, M. S. Kumar, Experimental and computational study of concrete filled steel tubular columns under axial loads. Journal of Constructional Steel Research. 63 (2007) 182-193.

[7] Z-W. Yu, F-X. Ding, C.S. Cai, Experimental behavior of circular concrete-filled steel tube stub columns. Journal of Constructional Steel Research, 63 (2007) 165-174.

[8] K.A.S. Susantha, G. Hanbin, Usami T, Uniaxial stress–strain relationship of concrete confined by various shaped steel tubes. Engineering Structures, 23 (2001) 1331-1347.

[9] W.L.A Oliveira, S. De Nardin, A.L.H. de C. El Debs, M.K. El Debs, evaluating passive confinement in CFT columns. Journal of Constructional Steel Research, 66 (2009) 487-495.

[10] X-F. Yan, Y-G. Zhao, S. Lin, H. Zhang. Confining stress path-based compressive strength model of axially compressed circular concrete-filled double-skin steel tubular short columns. Thin-Walled Structures, 165 (2021) 107949.

[11] G. Giakoumelis, D. Lam, Axial capacity of circular concrete-filled steel tube columns. Journal of Constructional Steel Research. 60 (2004) 1049-1068.

[12] ACI Committee 318, Building code requirements for structural concrete (ACI 318-95). Detroit: American Concrete Institute; 1995.

[13] Australia Standards AS3600 Reinforced concrete structures. Sydney: Standards Australia; 1994.

[14] Australia Standards AS4100 Steel structures. Sydney: Standards Australia; 1998.

[15] M.V. Chitawadagi, N.C. Mattur, S.M. Kulkarni, Axial strength of circular concrete-filled steel tube columns — DOE approach. Journal of Constructional Steel Research. 66 (2010) 1248-1260.

[16] Y-G. Zhao, X-F. Yan, S. Lin. Compressive strength of axially loaded circular hollow centrifugal concrete filled steel tubular short columns. Engineering Structures. 201 (2019) 109828.

[17] J.Y.R. Liew, M.X. Xiong, Design Guide for Concrete Filled Tubular Members with High Strength Materials - An Extension of Eurocode 4 Method to C90/105 Concrete and S550 Steel. Research Publishing Services. Singapore, 2015.

[18] J.Y. R. Liew, M. Xiong, D. Xiong. Design of Concrete Filled Tubular Beam-columns with High Strength Steel and Concrete. Structures 8 (2016) 213–226.

[19] B. Uy, M. Khan, Z. Tao, F. Mashiri, Behaviour and design of high strength steel-concrete filled columns. The 2013 World Congress on Advances in Structural Engineering and Mechanics (ASEM13), Jeju, Korea, 2013.

[20] X-F. Yan, M.F. Hassanein, F. Wang, M-N. He. Behaviour and design of high-strength concrete-filled rectangular ferritic stainless steel tubular (CFFSST) short columns subjected to axial compression. Engineering Structures. 242 (2021) 112611.

[21] L-H. Han, W. Li, R. Bjorhovde, Developments and advanced applications of concrete-filled steel tubular. Journal of Constructional Steel Research, 100 (2014) 211-228.

[22] C.S. Poon, Z.H. Shui, L. Lam H. Fok, S.C. Kou, Influence of moisture states of natural and recycled aggregates on the slump and compressive strength of concrete. Cement and Concrete Research, 34 (2004) 31-36.

[23] J. Xiao, J. Lia, Ch. Zhang, Mechanical properties of recycled aggregate concrete under uniaxial loading. Cement and Concrete Research, 35 (2005) 1187-1194.

[24] K. Konno, Y. Sato, T. Uedo, Mechanical property of recycled concrete under lateral confinement. Transactions of the Japan Concrete Institute, 20 (1998) 287-292.

[25] F. Wu, Y. Yang, Preliminary research on behavior of recycled aggregate concrete-filled steel stub columns. Journal of Fuzhou University, 33 (2005) 209-212.

[26] Y-F. Yang, L-H. Han, Experimental behaviour of recycled aggregate concrete filled steel tubular columns. Journal of Constructional Steel Research, 62 (2006) 1310–1324.

[27] J. Yang, On mechanical properties of confined recycled aggregate concrete. Master's degree Dissertation, Tongji University, Shangai, 2009.

[28] Z. Chen, J. Xu, J. Xue, Y. Su, Performance and calculations of recycled aggregate concrete-filled steel tubular (RACFST) short columns under axial compression. International Journal of Steel Structures, 14 (2014) 31–42.

[29] V.W.Y. Tam, Z-B. Wang, Z. Tao, Behaviour of recycled aggregate concrete filled stainless steel stub columns. Materials and Structures, 47 (2014) 293-310.

[30] Y. Wang, J. Chen, Y. Geng, Testing and analysis of axially loaded conventional-strength recycled aggregate concrete filled steel tubular stub columns. Engineering Structural, 86 (2015) 192-212.

[31] J-J. Xu, Z-P. Chen, T. Ozbakkaloglu, X-Y. Zhao, C. Demartino, A critical assessment of the compressive behavior of reinforced recycled aggregate concrete columns. Engineering Structures, 161 (2018) 161–175.

[32] A. Silva, Y. Jiang, J.M. Castro, N. Silvestre, R. Monteiro, Experimental assessment of the flexural behaviour of circular rubberised concrete-filled steel tubes. Journal of Constructional Steel Research 122 (2016) 557–570.

[33] A. Silva, Y. Jiang, J.M. Castro, N. Silvestre, R. Monteiro, Monotonic and cyclic flexural behaviour of square/rectangular rubberised concrete-filled steel tubes. Journal of Constructional Steel Research 139 (2017) 385-396.

[34] Z. Tao, T-Y. Song, B. Uy, L-H. Han, Bond behavior in concrete-filled steel tubes. Journal of Constructional Steel Research 120 (2016) 81-93.

[35] ABNT NBR 8800, Design of steel and composite structures for buildings. Associação Brasileira de Normas Técnicas, São Paulo, Brazil, 2008 (in Portuguese).

[36] ABNT NBR 16239, Design of steel and composite structures for buildings using hollow sections. Associação Brasileira de Normas Técnicas, São Paulo, Brazil, 2013 (in Portuguese).

[37] ABNT NBR 15116:2004, Recycled Aggregates of Solid Waste from Civil Construction - Use in Paving and Preparation of Concrete without Structural Function – Requirement. Associação Brasileira de Normas Técnicas. Rio de Janeiro, Brazil, 2004 (in Portuguese).

[38] American Institute of Steel Construction (AISC), Specification for Structural Steel Buildings. AISC 360-16, Chicago (IL), 2016.

[39] EN 1994-1-1:2004, Eurocode 4: Design of Composite Steel and Concrete Structures – Part 1-1: General Rules and Rules for Buildings, European Committee for Standardization (CEN), Brussels, 2004.

[40] AS/NZS 2327, Composite structures—Composite steel-concrete construction in buildings, Standards Australia, Sydney, Australia, 2017.

[41] V. da S. de Azevedo, Experimental evaluation of short columns CFST with recycled concrete core, PhD Thesis, PGECIV – Post Graduate Program in Civil Engineering, State University of Rio de Janeiro – UERJ, 2018 (in Portuguese).

[42] R.D. Zieman, Guide to Stability Design Criteria for Metal Structures. 6th Ed. John Wiley & Sons,1117p. 2010.

[43] Y. Huang, B. Young, The art of coupon tests. Journal of Constructional Steel Research, 96 (2014) 159–175.

[44] ABNT NBR 12655, Portland cement concrete - Preparation, control, receipt and acceptance - Procedure. ABNT NBR - Brazilian National Standards Organization. Rio de Janeiro, 2020 (in Portuguese).

[45] B. N. T. de. Macedo, Determination of the coefficient of superficial conformation of bars for use in reinforced concrete, MSc Dissertation, PGECIV – Post Graduate Program in Civil Engineering, State University of Rio de Janeiro – UERJ, 2018 (in Portuguese).

[46] ABNT NBR 7211, Recycled aggregate of solid residue of building constructions - Requirements and methodologies. ABNT NBR - Brazilian National Standards Organization. Rio de Janeiro, 2005 (in Portuguese)

[47] V.W.Y. Tam, C.M. Tam., Parameters for assessing recycled aggregate and their correlation, Waste Management & Research. 27 (2009) 52-58.

[48] R.V. Silva, J. de Brito, R.K. Dhir, The influence of the use of recycled aggregates on the compressive strength of concrete: a review, European Journal of Environmental and Civil Engineering. 19 (2015) 825-849.

[49] F. Wang, B. Young, L. Gardner, Compressive testing and numerical modelling of concrete-filled double skin CHS with austenitic stainless steel outer tubes. Thin-Walled Structures, 141 (2019) 345-359.